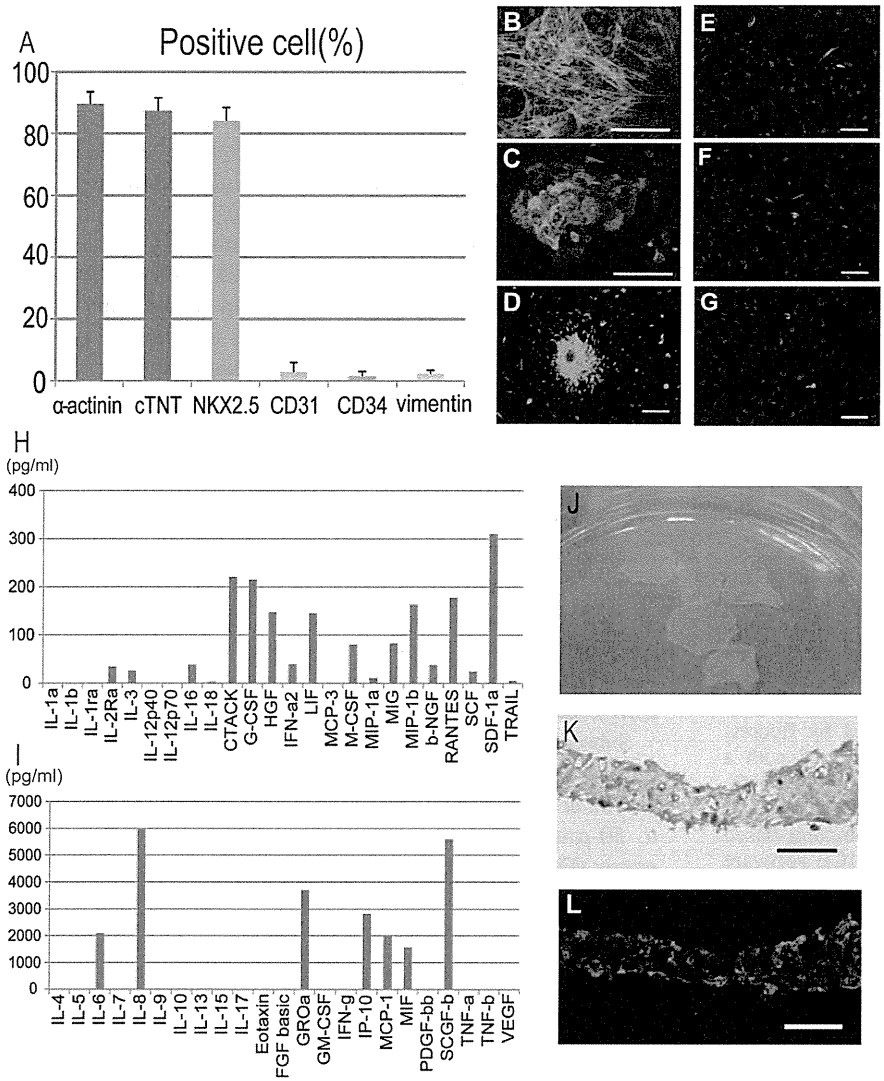

Figure 2. Histological characteristics of the hiPS-CM sheets. **A**, quantitative analysis of the numbers of hiPS-derived cells expressing α-actinin, cTNT, Nkx2.5, CD31, CD34, or vimentin, shown as percentages (%). Almost 90% pure cardiomyocytes were obtained. **B–G**, Immunostaining of the hiPS-CMs with anti-α-actinin (**B**), anticTNT (**C**), and anti-Nkx2.5 (**D**), anti-CD31 (**E**), anti-CD34 (**F**), and antivimentin (**G**) antibodies in green; bar=100 μm in **B–G. H–I**, In vitro screening for cytokines and growth factors. Several factors that may potentially be involved in cardiac repair were detected at relatively high concentrations in the medium. **J**, hiPS-CM sheets in a 10-cm dish. **K–L**, Hematoxylin and eosin (HE) staining (**K**) and immunostaining with cTNT antibody (**L**) of the hiPS-CM sheets in green. Many cTNT-positive cells were detected in the hiPS-CM sheets; bar=50 μm in **K–L**. The cell nuclei were counterstained with 4′,6-diamidino-2-phenylindole (DAPI) in blue (**B, C, E, F, G, L**). hiPS-CM indicates human induced pluripotent stem cell-derived cardiomyocyte.

end-systolic diameter was significantly smaller in the iPS group than in the sham group after 4 (25.0±1.9 mm versus 30.1±3.4 mm, $P<0.05$) and 8 (26.2±3.3 mm versus 34.7±5.4 mm, $P<0.05$) weeks, whereas LV end-diastolic diameter did not differ significantly between the 2 groups.

A cardiac multislice CT scan was performed 8 weeks after the treatment and also demonstrated that LVEF was significantly greater in the iPS group (50.7%±5.4%) than in the sham group (40.5%±1.7%, $P<0.05$; Figure 4A). LVEDV and LVESV were significantly smaller in the iPS group than in the sham group (57.1±7.5 mL versus 76.1±4.1 mL, $P<0.05$, and 28.3±6.0 mL versus 45.3±3.0 mL, $P<0.05$, respectively; Figure 4B–C).

Recovery of Regional LV Wall Motion After hiPS-CM Sheet Transplantation

Serial speckle-tracking echocardiography was performed to compare the strain values at baseline and 4 weeks after the treatment. Radial strain was measured from the midshort-axis plane to evaluate regional wall motion (Figure 5B–C). In the sham group, the radial strain levels in the infarct, the border, and the remote area had not changed significantly after 4 weeks relative to the baseline values. In contrast, in the iPS group, the radial strain in the border area was significantly greater after 4 weeks than at baseline (10.35%±4.17% versus 15.22%±1.66%, $P<0.05$), whereas the radial strain levels in the infarct and the remote area had not changed significantly.

Pathological Hypertrophy, Interstitial Fibrosis, and Vascular Density

The pathological cardiomyocyte hypertrophy, interstitial fibrosis, and vascular density 8 weeks after the treatment were assessed semiquantitatively by periodic acid-Schiff staining, picrosirius red staining, and immunohistochemistry for von Willebrand factor, respectively (Figure 6). The diameters of the cardiomyocytes in the remote area were significantly smaller in the iPS group than in the sham group. There was consistently significantly less accumulation of interstitial fibrosis in the remote area in the iPS group than in the sham group. In addition, the vascular density in the border area was significantly greater in the iPS group than in the sham group.

Upregulation of Vascular Endothelial Growth Factor and Basic Fibroblast Growth Factor Expression in the Border Area After Treatment

The expression levels of growth factors that are expressed in the myocardium and are potentially related to neovascular-

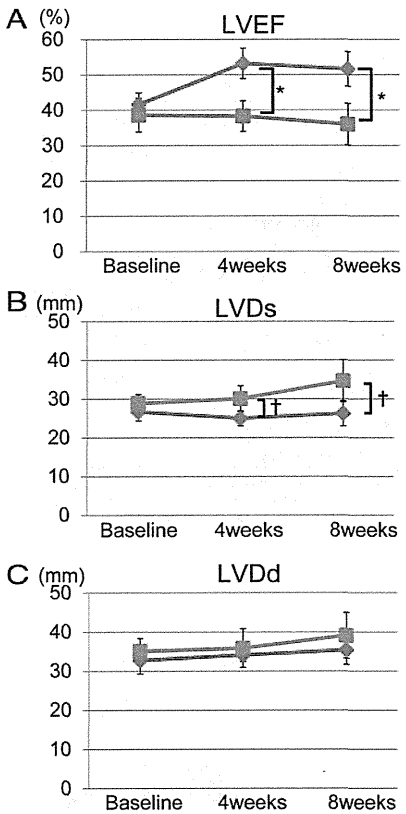

Figure 3. Echocardiographic evaluation. **A**, The global cardiac function as assessed by left ventricular ejection fraction (LVEF) was significantly better in the iPS group. **B**, The left ventricular end-systolic diameter (LVDs) was significantly smaller in the iPS group than in the sham group. **C**, The left ventricular end-diastolic diameter (LVDd) did not differ significantly between the iPS and sham groups. *$P<0.01$, †$P<0.05$ versus sham. The red line indicates the iPS group and the blue line the sham group. iPS indicates induced pluripotent stem cells.

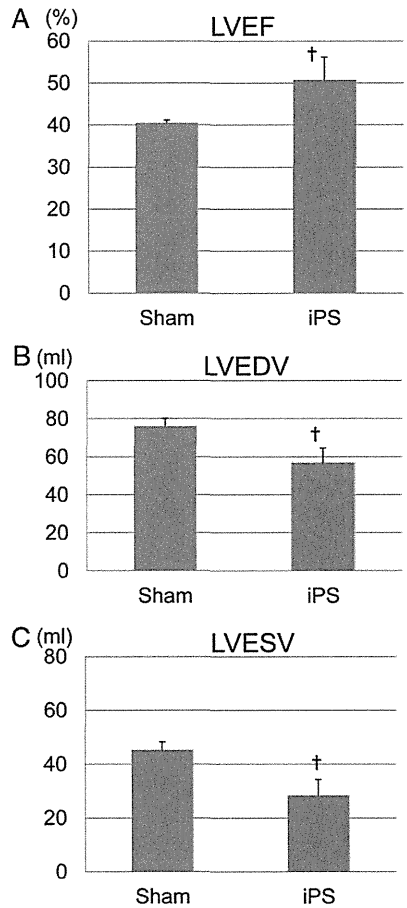

Figure 4. Cardiac multislice CT analysis. **A**, The global cardiac function as assessed by LVEF was significantly better in the iPS group. **B–C**, The left ventricular end-diastolic (LVEDV; **B**) and end-systolic (LVESV; **C**) volumes were significantly smaller in the iPS group than in the sham group. †$P<0.05$ versus sham. LVEF indicates left ventricular ejection fraction; iPS, induced pluripotent stem cells.

ization were quantified by real-time polymerase chain reaction 8 weeks after the treatment. The expression levels of vascular endothelial growth factor and basic fibroblast growth factor in the border area were significantly greater in the iPS group than in the sham group (Figure 7).

Phenotypic Fate of the Transplanted iPS-CMs in the Heart

The hiPS-CMs were labeled in vitro with a red fluorescent marker before transplantation. The labeled cells were identified on the surface of the heart 2 weeks after transplantation. Some of these cells were positive for slow myosin heavy chain (Figure 8A–D). Because the labeled cells could no longer be identified by 8 weeks after transplantation, the presence of the transplanted cells was assessed by fluorescence in situ hybridization using a human-specific genomic probe 8 weeks after transplantation. A small number of human genome-positive cells that expressed slow myosin heavy chain remained present in the infarct area (Figure 8E–G).

Discussion

The major findings of this study were as follows: (1) the newly developed culture system for hiPS cells successfully yielded approximately 2.5×10^7 highly pure hiPS-CMs, and hiPS-CM sheets could be made from these high pure hiPS-CMs using temperature-responsive dishes; (2) the hiPS-CM sheets survived in damaged myocardium in the short term and improved cardiac function in a porcine ischemic cardiomyopathy model, chiefly through the paracrine effects of cytokines. Histological analysis indicated that transplantation of hiPS sheets attenuated left ventricular remodeling and increased neovascularization; and (3) hiPS-derived cardiomyocytes could still be detected 8 weeks after transplantation, but the number of hiPS-CMs that survived long term was very small. No teratoma formation was observed in animals that received hiPS-CM sheets.

The optimal number of cells for clinical use of cardiac regeneration therapy remains unknown. Implantation of approximately 10^8 to 10^9 cells was shown to produce cardiac improvement in previous clinical trials using bone marrow-derived cells.[16] Given these results, it may be necessary to transplant almost this number of hiPS-CMs into impaired myocardium to improve cardiac function in a clinical setting. It is challenging to obtain large numbers of hiPS-CMs at high purity because clinical application of hiPS cells requires 3 steps (ie, proliferation, differentiation, and purification). In

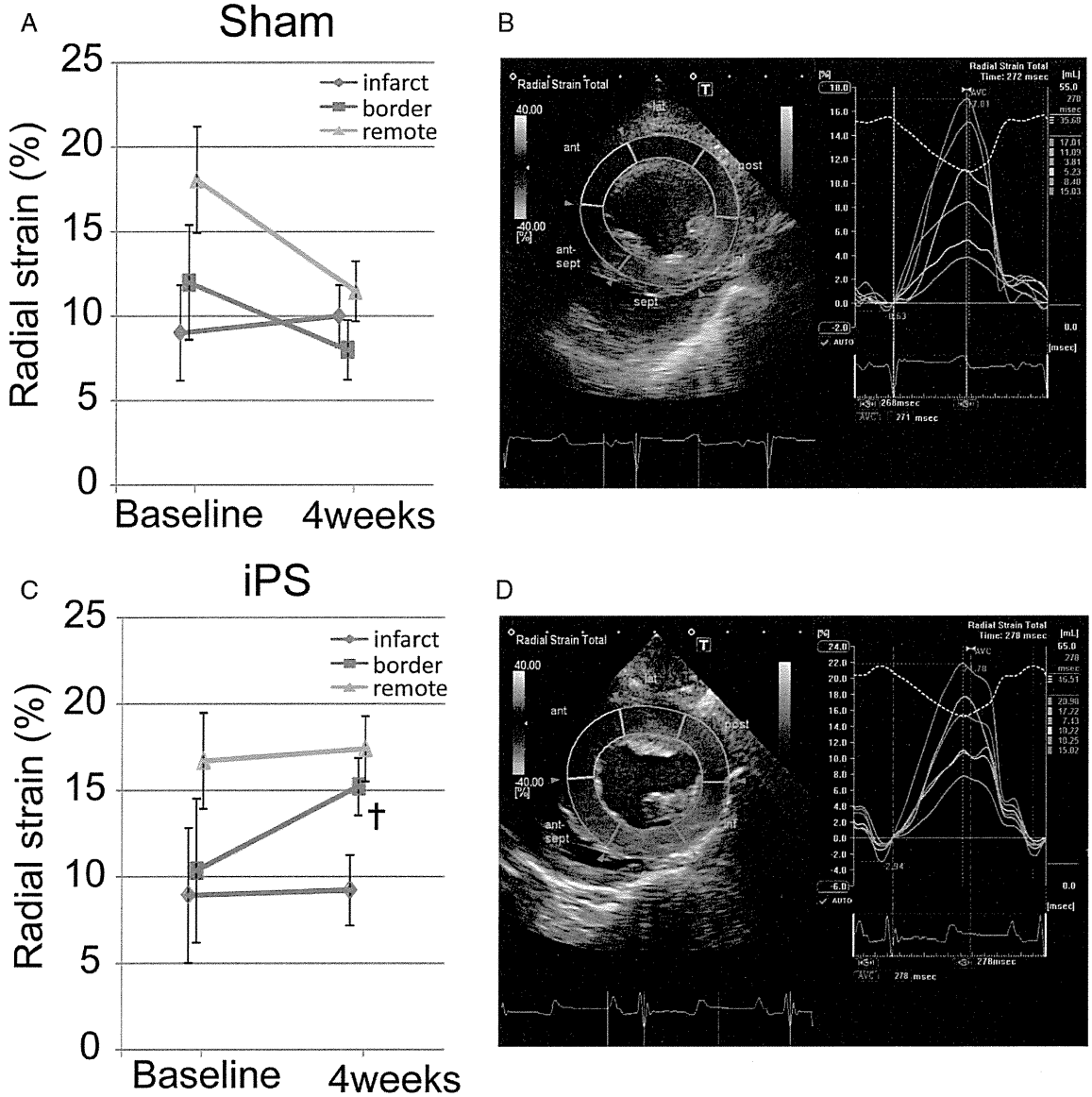

Figure 5. Evaluation of regional wall motion by 2-dimensional speckle-tracking echocardiography. Representative examples of radial strain analysis in each group are shown in **B** (sham) and **D** (iPS). **A**, In the sham group, the radial strain values of all areas did not differ significantly between the baseline and 4 weeks after the sham operation. **C**, In the iPS group, the radial strain value of the border area of the infarct was significantly greater 4 weeks after treatment than at baseline. The radial strain values of the other areas relative to the infarct did not differ significantly before and after hiPS-CM-sheet transplantation. †$P<0.05$ versus baseline. iPS indicates induced pluripotent stem cells; hiPS-CM, human induced pluripotent stem cell-derived cardiomyocyte.

the present study, we obtained approximately 2.5×10^7 hiPS-CMs after differentiation and purification of hiPS cells. One advantage of our culture system for hiPS cells its simplicity, because it involves only supplementation with cytokines for differentiation and culture in glucose-free medium for purification. Our culture system might be able to yield higher numbers of hiPS-CMs and could, possibly, be expanded to a clinically useful scale. Moreover, a previous study evaluating the propensity of secondary neurospheres generated from iPS cells to form teratomas found a significant correlation between the teratoma diameter and the proportion of undifferentiated cells in the secondary neurospheres.[17] Importantly, no teratoma formation was detected in the current experiment, which could be because our purification method limited the number of undifferentiated iPS cells in the hiPS-CMs.

Structural connection and electromechanical integration have been considered to be the mechanisms of functional recovery of the impaired myocardium after ES cell-derived cardiomyocyte transplantation.[18,19] We therefore predicted that the hiPS-CMs would connect structurally and electromechanically with the host myocardium, as seen for ES cell-derived cardiomyocytes. However, although functional cardiac recovery was observed after hiPS-CM-sheet transplantation, only a few transplanted cells were persistently present. It has been shown that the therapeutic effects of stem cell therapy can result from paracrine or direct effects. Paracrine effects have been considered as the major mechanisms responsible for the therapeutic efficacy of cell therapy with somatic tissue-derived stem or progenitor cells. These effects classically refer to the ability of transplanted cells to extracellularly

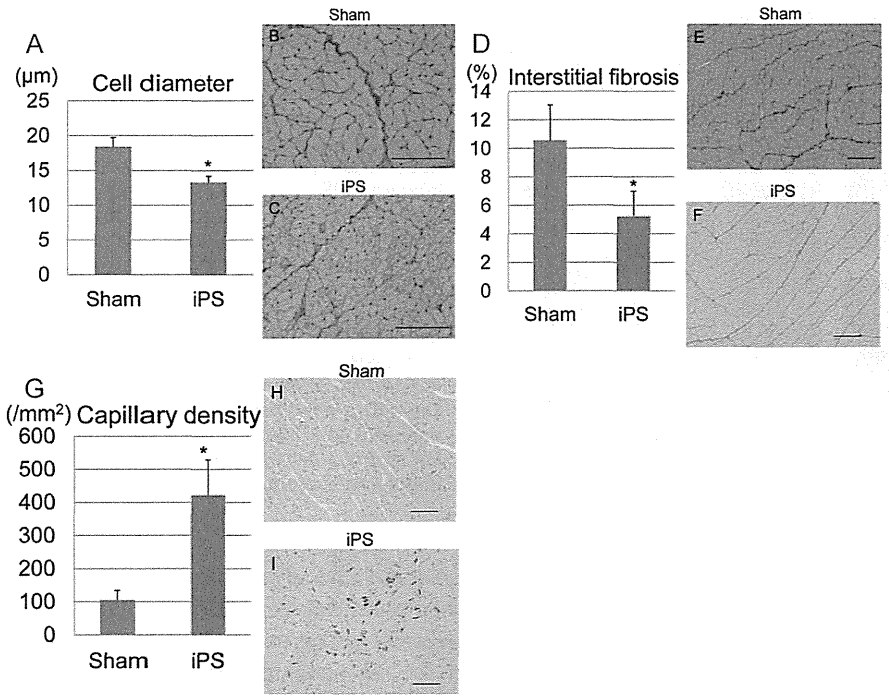

Figure 6. Histological evaluation after hiPS-CM-sheet transplantation. **A–C**, The diameters of the cardiomyocytes were measured at an area remote from the infarct; cardiomyocyte hypertrophy was significantly lower in the iPS group than in the sham group (**A**). Photomicrographs of periodic acid-Schiff (PAS)-stained sections are shown in **B–C**. **D–F**, The proportions of fibrosis-occupied area (%) at a site remote from the infarct; Picrosirius red staining demonstrated significantly less interstitial fibrosis in the iPS group than in the sham group (**D**). Photomicrographs of the Picrosirius red-stained sections are shown in **E–F**. **G–I**, Capillary density in an area bordering the infarct; the capillary density as assessed by immunostaining with an anti-von Willebrand factor antibody was significantly better in the iPS group (**G**). Photomicrographs of immunostaining for von Willebrand factor are shown in **H–I**. *$P<0.01$ versus sham. Bar=100 μm. hiPS-CM indicates human induced pluripotent stem cell-derived cardiomyocyte; iPS, induced pluripotent stem cells.

release various cardioprotective factors into the damaged cardiac tissue to directly enhance reverse LV remodeling. In contrast, recent reports have suggested that cell transplantation upregulates various cardioprotective factors native to the cardiac tissue through "crosstalk" between the transplanted cells and the native cardiac tissue.[2,20] In addition, another report has shown that paracrine effects of human cardiosphere-derived cells, which are capable of directed cardiac regeneration in vivo, play important roles in improving infarcted myocardium.[21] In our study, we observed that several factors, which were reportedly involved in cardiac repair,[20] were secreted by hiPS-CMs during in vitro screening. Consequently, cardiomyocyte hypertrophy and interstitial fibrosis were significantly attenuated in the infarct-remote area after cell sheet transplantation. In addition, capillary density was increased in the infarct border area associated with the upregulation of vascular endothelial growth factor and basic fibroblast growth factor after cell sheet transplantation. Speckle-tracking echocardiography showed that the regional function in the corresponding area was preserved after cell sheet transplantation as compared with that after a sham operation, in which the regional function progressively deteriorated. This suggests that ischemia-related hibernation in the infarct border myocardium might have recovered by increased blood flow because of angiogenesis. These findings suggest that in our study, paracrine effects are the major mechanisms underlying the functional improvement after hiPS-CM-sheet implantation. In contrast, only a small fraction of the transplanted cells differentiated into cardiac lineage, as assessed by fluorescence in situ hybridization analysis, which clearly distinguished cells of human origin from porcine cardiac tissue. This finding suggests that direct effects were not a major contributing mechanism responsible for the functional benefits observed in this study. Therefore,

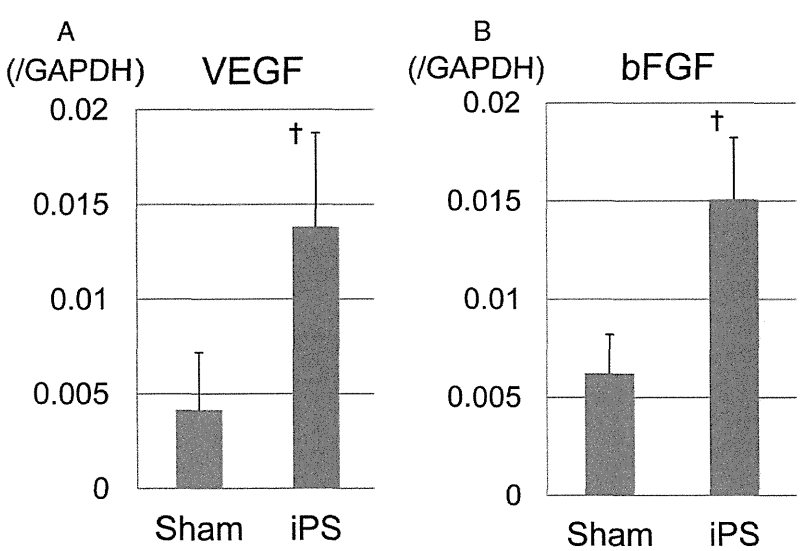

Figure 7. Neovascularization-related mRNA expression in an area bordering the infarct measured by real-time polymerase chain reaction (RT-PCR). The mRNA expression levels of vascular endothelial growth factor (VEGF; **A**) and basic fibroblast growth factor (bFGF; **B**) were significantly higher in the iPS group than in the sham group. †$P<0.05$ versus sham. iPS indicates induced pluripotent stem cells.

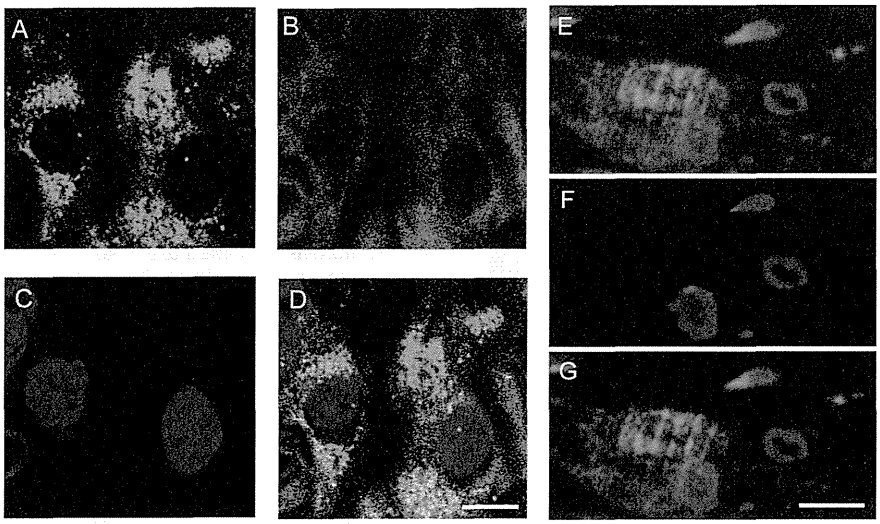

Figure 8. The hiPS-CMs in the heart after transplantation. **A–D**, Detection of red fluorescence-labeled hiPS-CMs 2 weeks after transplantation; representative photomicrographs showing slow myosin heavy chain (sMHC) in green (**A**) and labeled hiPS-CMs in red (**B**). **E–G**, Detection of hiPS-CMs 8 weeks after transplantation by fluorescence in situ hybridization (FISH) using a human-specific genomic probe; immunostaining for sMHC is shown in green (**E**) and positive FISH signals in red (**F**). The nuclei were stained with DAPI in blue (**C, E, F**). Merged images are shown in **D** and **G**. Bar=10 μm in **D** and **G**. hiPS-CM indicates human induced pluripotent stem cell-derived cardiomyocyte; DAPI, 4′,6-diamidino-2-phenylindole dihydrochloride.

it will be important to develop additive treatment to enhance survival, differentiation, and integration of the transplanted cells into the cardiac tissue.

Histological analysis revealed that most of the implanted hiPS-CMs disappeared after implantation, indicating poor engraftment of the hiPS-CMs into the impaired myocardium. In our study, hiPS-CMs secreted multiple angiogenic factors or their inducers, and the hiPS-CMs included small populations of CD31- or CD34-positive cells. These findings indicate that the hiPS-CM sheets have angiogenic potential, which might result in the generation of new vascular networks between the hiPS-CM sheets and the host cardiac tissue. A previous report has shown that the prompt formation of a vascular network between the cell sheet and the surrounding host tissue can sufficiently supply blood and oxygen to the transplanted cell sheet to survive and function in the host tissue.[22] However, in the present study, the host myocardium persistently experienced low blood supply due to coronary artery occlusion, which can interfere with the formation of a new vascular network between the cardiac tissue and the transplanted hiPS-CM sheets, possibly leading to poor survival and differentiation of the transplanted cells in the heart. Poor engraftment has been shown after experimental transplantation of human ES cell-derived cardiomyocytes through simple injection into the infarcted myocardium; treatment with several factors that block cell death pathways improved the engraftment of transplanted ES cell-derived cardiomyocytes.[23] We recently established a new method of cell protection by gene transfection[24] and a novel cell delivery system using the omentum,[25] which can enhance the therapeutic effects of cell therapy. Additional methods of prolonging cell survival after implantation might be necessary to improve the engraftment rate and thus obtain long-standing therapeutic effects of the hiPS-CM sheet from not only paracrine factors, but also direct contributions to the host heart.

Successful regeneration therapy using human pluripotent stem cells requires that the stem cells or their derivatives remain in the recipient myocardium long term. Unless the cell transplantation is autogeneic, the cells will inevitably be rejected by the immune system. Future clinical applications of hiPS cells for regeneration therapy may involve allogeneic and HLA type-matched transplantations, because some acute injuries such as myocardial infarction, stroke, or spinal cord trauma are targeted for regeneration therapy.[26] Therefore, elimination of immunologic rejection or induction of immunologic tolerance of the transplanted stem cells or their derivatives is a critical issue in stem cell-based medicine.[27] In the present study, we used tacrolimus as the only immunosuppressant in a xenotransplantation model; therefore, the failure of prolonged engraftment of hiPS-CMs could have been due to insufficient immunosuppressive therapy. A previous study has demonstrated that combined therapy with tacrolimus and sirolimus significantly prolonged the survival of human ES cells in a xenotransplantation model.[28] In another experiment, blocking the leukocyte costimulatory molecules was found to promote successful engraftment of ES and iPS cells in allogeneic and xenogeneic transplantation models.[26] These findings indicate that appropriate immunosuppressive therapies could improve stem cell engraftment. However, the immunogenicity of iPS cells has not yet been fully investigated. Further studies are needed to establish appropriate strategies for inducing and maintaining immunologic tolerance during the clinical use of allogeneic iPS cell therapy.

In conclusion, the present study showed that our culture system yields a large number of highly pure hiPS-CMs and that hiPS-CM sheets could improve cardiac function in the context of ischemic cardiomyopathy, primarily through paracrine cytokine effects. This newly developed culture system and the hiPS-CM sheets may provide a basis for clinical hiPS-CM-sheet transplantation as part of a strategy for promoting the regeneration of damaged myocardium.

Acknowledgments

We thank Shigeru Matsumi, Masako Yokoyama, and Akima Harada for excellent technical assistance.

Disclosures

Dr Shimizu is a consultant for CellSeed, Inc. Dr Okano is an Advisory Board Member in CellSeed, Inc, and an inventor/developer designated on the patent for temperature-responsive culture surfaces.

References

1. Jessup M, Brozena S. Heart failure. *N Engl J Med.* 2003;348:2007–2018.
2. Gonzales C, Pedrazzini T. Progenitor cell therapy for heart disease. *Exp Cell Res.* 2009;315:3077–3085.
3. Takahashi K, Yamanaka S. Induction of pluripotent stem cells from mouse embryonic and adult fibroblast cultures by defined factors. *Cell.* 2006;126:663–676.
4. Takahashi K, Tanabe K, Ohnuki M, Narita M, Ichisaka T, Tomoda K, Yamanaka S. Induction of pluripotent stem cells from adult human fibroblasts by defined factors. *Cell.* 2007;131:861–872.
5. Yu J, Vodyanik MA, Smuga-Otto K, Antosiewicz-Bourget J, Frane JL, Tian S, Nie J, Jonsdottir GA, Ruotti V, Stewart R, Slukvin II, Thomson JA. Induced pluripotent stem cell lines derived from human somatic cells. *Science.* 2007;318:1917–1920.
6. Germanguz I, Sedan O, Zeevi-Levin N, Shtrichman R, Barak E, Ziskind A, Eliyahu S, Meiry G, Amit M, Itskovitz-Eldor J, Binah O. Molecular characterization and functional properties of cardiomyocytes derived from human inducible pluripotent stem cells. *J Cell Mol Med.* 2011;15:38–51.
7. Ren Y, Lee MY, Schliffke S, Paavola J, Amos PJ, Ge X, Ye M, Zhu S, Senyei G, Lum L, Ehrlich BE, Qyang Y. Small molecule Wnt inhibitors enhance the efficiency of BMP-4-directed cardiac differentiation of human pluripotent stem cells. *J Mol Cell Cardiol.* 2011;51:280–287.
8. Yamashita JK. ES and iPS cell research for cardiovascular regeneration. *Exp Cell Res.* 2010;316:2555–2559.
9. Yoshida Y, Yamanaka S. iPS cells: a source of cardiac regeneration. *J Mol Cell Cardiol.* 2011;50:327–332.
10. Masuda S, Shimizu T, Yamato M, Okano T. Cell sheet engineering for heart tissue repair. *Adv Drug Deliv Rev.* 2008;60:277–285.
11. Memon IA, Sawa Y, Fukushima N, Matsumiya G, Miyagawa S, Taketani S, Sakakida SK, Kondoh H, Aleshin AN, Shimizu T, Okano T, Matsuda H. Repair of impaired myocardium by means of implantation of engineered autologous myoblast sheets. *J Thorac Cardiovasc Surg.* 2009;130:646–653.
12. Miyagawa S, Saito A, Sakaguchi T, Yoshikawa Y, Yamauchi T, Imanishi Y, Kawaguchi N, Teramoto N, Matsuura N, Iida H, Shimizu T, Okano T, Sawa Y. Impaired myocardium regeneration with skeletal cell sheets. A preclinical trial for tissue-engineered regeneration therapy. *Transplantation.* 2010;90:364–372.
13. Jaroszeski MJ, Gilbert R, Heller R. Detection and quantitation of cell–cell electrofusion products by flow cytometry. *Anal Biochem.* 1994;216:271–275.
14. Teramoto N, Koshino K, Yokoyama I, Miyagawa S, Zeniya T, Hirano Y, Fukuda H, Enmi J, Sawa Y, Knuuti J, Iida H. Experimental pig model of old myocardial infarction with long survival leading to chronic left ventricular dysfunction and remodeling as evaluated by PET. *J Nucl Med.* 2011;52:761–768.
15. Teichholz LE, Kreulen T, Herman MV, Gorlin R. Problems in echocardiographic volume determinations: echocardiographic–angiographic correlations in the presence or absence of asynergy. *Am J Cardiol.* 1976;37:7–11.
16. Rosenzweig A. Cardiac cell therapy—mixed results from mixed cells. *N Engl J Med.* 2006;355:1274–1277.
17. Miura K, Okada Y, Aoi T, Okada A, Takahashi K, Okita K, Nakagawa M, Koyanagi M, Tanabe K, Ohnuki M, Ogawa D, Ikeda E, Okano H, Yamanaka S. Variation in the safety of induced pluripotent stem cell lines. *Nat Biotechnol.* 2009;27:743–745.
18. Caspi O, Huber I, Kehat I, Habib M, Arbel G, Gepstein A, Yankelson L, Aronson D, Beyar R, Gepstein L. Transplantation of human embryonic stem cell-derived cardiomyocytes improves myocardial performance in infarcted rat hearts. *J Am Coll Cardiol.* 2007;50:1884–1893.
19. Kehat I, Khimovich L, Caspi O, Gepstein A, Shofti R, Arbel G, Huber I, Satin J, Itskovitz-Eldor J, Gepstein L. Electromechanical integration of cardiomyocytes derived from human embryonic stem cells. *Nat Biotechnol.* 2004;22:1282–1289.
20. Gnecchi M, Zhang Z, Ni A, Dzau VJ. Paracrine mechanisms in adult stem cell signaling and therapy. *Circ Res.* 2008;103:1204–1219.
21. Chimenti I, Smith RR, Li TS, Gerstenblith G, Messina E, Giacomello A, Marbán E. Relative roles of direct regeneration versus paracrine effects of human cardiosphere-derived cells transplanted into infarcted mice. *Circ Res.* 2010;106:971–980.
22. Shimizu T, Sekine H, Yang J, Isoi Y, Yamato M, Kikuchi A, Kobayashi E, Okano T. Polysurgery of cell sheet grafts overcomes diffusion limits to produce thick, vascularized myocardial tissues. *FASEB J.* 2006;20:708–710.
23. Laflamme MA, Chen KY, Naumova AV, Muskheli V, Fugate JA, Dupras SK, Reinecke H, Xu C, Hassanipour M, Police S, O'Sullivan C, Collins L, Chen Y, Minami E, Gill EA, Ueno S, Yuan C, Gold J, Murry CE. Cardiomyocytes derived from human embryonic stem cells in prosurvival factors enhance function of infarcted rat hearts. *Nat Biotechnol.* 2007;25:1015–1024.
24. Miyagawa S, Sawa Y, Taketani S, Kawaguchi N, Nakamura T, Matsuura N, Matsuda H. Myocardial regeneration therapy for heart failure: hepatocyte growth factor enhances the effect of cellular cardiomyoplasty. *Circulation.* 2002;105:2556–2561.
25. Shudo Y, Miyagawa S, Fukushima S, Saito A, Shimizu T, Okano T, Sawa Y. Novel regenerative therapy using cell-sheet covered with omentum flap delivers a huge number of cells in a porcine myocardial infarction model. *J Thorac Cardiovasc Surg.* 2011;142:1188–1196.
26. Pearl JI, Lee AS, Leveson-Gower DB, Sun N, Ghosh Z, Lan F, Ransohoff J, Negrin RS, Davis MM, Wu JC. Short-term immunosuppression promotes engraftment of embryonic and induced pluripotent stem cells. *Cell Stem Cell.* 2011;8:309–317.
27. Chidgey AP, Layton D, Trounson A, Boyd RL. Tolerance strategies for stem-cell-based therapies. *Nature.* 2008;453:330–337.
28. Swijnenburg RJ, Schrepfer S, Govaert JA, Cao F, Ransohoff K, Sheikh AY, Haddad M, Connolly AJ, Davis MM, Robbins RC, Wu JC. Immunosuppressive therapy mitigates immunological rejection of human embryonic stem cell xenografts. *Proc Natl Acad Sci U S A.* 2008;105:12991–12996.

Supplemental Materials

MS ID#: CIRCULATIONAHA/2011/084343

Feasibility, Safety, and Therapeutic Efficacy of Human Induced Pluripotent Stem Cell-derived Cardiomyocyte Sheets in a Porcine Ischemic Cardiomyopathy Model

Materials and Methods

All experimental procedures were approved by the institutional ethics committee. Animal care was conducted humanely in compliance with the "Principles of Laboratory Animal Care" formulated by the National Society for Medical Research and the "Guide for the Care and Use of Laboratory Animals" prepared by the Institute of Animal Resources and published by the National Institutes of Health (Publication No 85-23, revised 1996).

Culture, differentiation, and purification of human iPS cells and collection of conditioned medium

The human iPS (hiPS) cell line 201B7 that was generated using the 4 transcription factors Oct4, Sox2, Klf4, and c-Myc (a generous gift from Professor Yamanaka, Kyoto University, Japan) was used in this study[1]. The hiPS cells were cultured on matrigel™ (BD Bioscience, San Jose, CA)-coated dishes in mTeSR1 medium (Stem Cell Technologies, Vancouver, BC, Canada) that was changed daily. Human iPS cells were then dissociated using StemPro® Accutase® Cell

Dissociation Reagent (Invitrogen, Carlsbad, CA), transferred to Corning® ultra-low-attachment surface culture dishes (Sigma-Aldrich Corp., St. Louis, MO) at a density of 50,000 cells/mL in mTeSR1 with Y-27632 (Wako Pure Chemical Industries, Osaka, Japan), and cultured for 4 days to allow them to form embryoid bodies (EBs). The EBs were re-plated with differentiation medium (DM; DMEM-F12, Invitrogen) containing 20% fetal bovine serum (FBS), 100 μM nonessential amino acids (Invitrogen), 50 U/mL penicillin, 50 mg/mL streptomycin (Invitrogen), and 5.5 mM 2-mercaptoethanol (Invitrogen) and supplemented with 100 ng/mL Wnt3a (R&D Systems, Minneapolis, MN) and 100 ng/mL R-Spondin-1 (Stem RD, Burlingame, CA) and cultured for 2 days. The culture medium was then replaced with DM without the supplemental factors for 2 days and then changed to DM supplemented with 100 ng/mL Dkk1 (R&D Systems) for 2 days. On day 10, the EBs were plated on gelatin-coated dishes in DM, which was refreshed every 2 days.

The culture medium was subsequently replaced with glucose-free DMEM (Invitrogen) with 1 mM lactic acid (Wako) (Hattori, F. and Fukuda, K. WO2007/088874; PCT/JP2007/051563, 2007) on day 20 and changed to DMEM/10% FBS the next day. On day 25, the culture medium was again replaced with glucose-free DMEM with 1 mM lactic acid and changed to DMEM/10% FBS the next day; this procedure eventually generated pure hiPS cell-derived cardiomyocytes (hiPS-CM). The hiPS-CMs were then labeled with a red fluorescent marker (CellTracker Red CMTPX, Invitrogen), as previously described[2]. FBS-free DMEM media were conditioned by hiPS-CMs for 48 hours after the completion of our differentiation and purification protocols. A total

of 48 cytokines and growth factors were measured by the Bio-Plex human cytokine assay (Bio-Rad, UK) for *in-vitro* screening.

Preparation of hiPS cell-derived cardiomyocyte sheets

The hiPS-CMs were detached using StemPro® Accutase® Cell Dissociation Reagent and seeded onto 6-cm UpCell dishes (CellSeed, Tokyo, Japan) at a density of 4×10^6 cells/dish in combination with normal human dermal fibroblasts (NHDF; Lonza, Basel, Switzerland) at 8×10^5 cells/dish. The next day, the dish was incubated at room temperature, which caused the cells to detach spontaneously to form a scaffold-free hiPS-CMs sheet.

Generation of the porcine chronic myocardial infarction model

Twelve female mini-pigs (Japan Farm, Kagoshima, Japan) weighing 20 to 25 kg were pre-anesthetized with ketamine hydrochloride (20 mg/kg, DAIICHI SANKYO, Tokyo, Japan) and xylazine (2 mg/kg, Bayer HealthCare, Leverkusen, Germany), intubated endotracheally (6 Fr Sheridan, InterMed Japan, Osaka, Japan), and maintained under general anesthesia by a continuous infusion of propofol (6 mg/kg/h, Astra-Zeneca) and vecuronium bromide (0.05 mg/kg/h), DAIICHI SANKYO). The pericardial space was exposed by left thoracotomy through the fourth intercostal space. The distal portion of the left anterior descending coronary artery (LAD) was ligated directly, and an ameroid constrictor (COR-2.50-SS, Research Instruments) was placed

around the LAD just distal to the branch point of the left circumflex coronary artery[3]. The muscle and skin were closed in layers, and the mini-pigs were then allowed to recover and maintained in temperature-controlled individual cages for 4 weeks.

Transplantation of hiPS-CMs sheets

All animals were immunosuppressed by daily administration of tacrolimus (0.6 mg/kg, Astellas, Tokyo, Japan) from 5 days before transplantation until sacrifice. Four weeks after the ameroid placement, the mini-pigs were randomly divided into 2 treatment groups (n = 6 each) to undergo either hiPS-CMs sheet transplantation (iPS group) or sham operation.

The hiPS-CMs sheets were transplanted via median sternotomy under general anesthesia. The area of the myocardial infarct was identified visually on the basis of surface scarring and abnormal wall motion. In the iPS group, 8 hiPS-CM sheets were transplanted over the infarcted myocardium. Two layers of hiPS-CM sheets were stacked over the broad surface of the myocardium. The mini-pigs were then allowed to recover in temperature-controlled individual cages and were later humanely sacrificed for analysis. The excised heart and other thoracic organs were visually inspected for possible tumor formation.

Standard and 2D speckle-tracking echocardiography

Transthoracic echocardiography was performed under general anesthesia using a 5.0-MHz transducer (Aplio Artida; Toshiba, Otawara, Japan). The left ventricular (LV) end-diastolic and end-systolic diameters (LVDd and LVDs, respectively) were measured in M-mode in the short-axis view, while the LV end-diastolic and end-systolic volumes (LVEDV and LVESV, respectively) were calculated from the Teichholz formula[4]. The LV ejection fraction (LVEF) was calculated from the following formula: LVEF (%) = 100 × (LVEDV - LVESV)/(LVEDV). The data are presented as the average of the measurements over 3 continuous beats.

Two-dimensional speckle-tracking echocardiography (2DSE) analysis was performed using the customized 2DSE software for the Toshiba system (2D Wall Motion Tracking, Toshiba Medical Systems). The endocardial border was traced manually, and a region of interest was drawn to include the entire myocardium. The software algorithms automatically segmented the LV planes into equidistant segments and performed speckle tracking on a frame-to-frame basis. The studies were assessed visually, and abnormal curves that appeared to be artifactual were excluded. Regional cardiac function was evaluated using radial strain values obtained from the mid-short-axis plane. The anterior and anteroseptal segments were defined as the infarct area, while the lateral and inferoseptal segments were defined as the border area and the posterior and inferior segments as the remote area. The strain value of each area was calculated from the average of 2 segments and expressed as a percentage (%).

Cardiac computed tomography scan

Electrocardiogram-gated multislice computed tomography (MSCT) was performed under general anesthesia in the supine position during end-expiratory breathhold with a 16-slice MSCT scanner (Somatron Emotion 16, Siemens, Forchheim, Germany). A standardized examination protocol was applied using 16 × 0.75-mm collimation, a 3.4-mm table feed per rotation, and a tube rotation time of 420 ms. The tube voltage was 120 kV with 500 effective mAs. MSCT was performed after intravenous injection of 90 mL of non-ionic contrast medium (Iomeprol, Bracco Imaging, Konstanz, Germany). Axial images were reconstructed using the scanner software. All images were analyzed on a workstation (AZE, Virtual Place Lexus 64). LVEDV and LVESV were obtained from the workstation and LVEF was calculated using the formula described above.

Holter electrocardiogram

Holter electrocardiogram (ECG) was performed for 24 hours in both groups (n = 6 each). The arrhythmogenesis associated with hiPS-CMs sheet transplantation was evaluated based on the number of premature ventricular contractions.

Histology and immunohistolabeling

Dissociated cultured cells were fixed in 4% paraformaldehyde for 20 minutes at room temperature, washed 3 times with phosphate-buffered saline (PBS), permeabilized with 0.2% Triton X-100 for

30 minutes, and blocked with 3% BSA in PBS for 2 hours. The primary antibodies used included anti-cardiac troponin T (cTNT, 1:100 dilution, Abcam, Cambridge, UK), anti-Nkx2.5 (1:100 dilution, Santa Cruz Biotechnology, Santa Cruz, CA), anti-α-actinin (1:100 dilution, Sigma-Aldrich Corp.), anti-human CD31 (1:100 dilution, BD Biosciences, San Jose, CA), anti-human CD34 (1:100 dilution, BD Biosciences), and anti-vimentin (1:100 dilution, BD Biosciences) and were visualized by fluorophore-conjugated secondary antibodies such as AlexaFluor488 goat anti-rabbit IgG, AlexaFluor488 goat anti-mouse IgG, and AlexaFluor488 donkey anti-goat IgG (1:1000 dilution, Invitrogen) with counterstaining by 4′,6-diamidino-2-phenylindole (DAPI, Dojindo, Tokyo, Japan) and assessed by fluorescence microscopy. Images of the samples were acquired with a Biorevo BZ-9000 (Keyence, Osaka, Japan). Positivity of the cardiomyocyte-specific markers or other lineage markers in the cultured cells was determined from the acquired images by using computer-based cell counting with the Dynamic Cell Count BZ-H1CE software (Keyence).

The excised heart specimens were either fixed with 10% buffered formalin and embedded in paraffin or fixed with 4% paraformaldehyde, embedded in OCT compound (Tissue Tek; Sakura Finetek, Torrance, CA), and snap-frozen. The paraffin-embedded sections were stained with Picrosirius red or periodic acid-Schiff (PAS) to assess interstitial fibrosis and cardiomyocyte hypertrophy, respectively[5,6]. The paraffin-embedded sections were immunolabeled with anti-human von Willebrand factor antibody (Dako, Glostrup, Denmark) and visualized with the horseradish peroxidase-based EnVision kit (Dako) according to the manufacturer's instructions.

Ten different fields were randomly selected, and the number of stained vascular endothelial cells in each field was counted using a light microscope under high-power magnification (×200). The stained blood vessels from the 10 fields were averaged and the results expressed as vascular density (per square millimeter). The frozen sections were immunolabeled with primary antibodies, such as anti-cTNT (Abcam) and anti-slow myosin heavy chain (sMHC, Sigma-Aldrich Corp.), visualized with AlexaFluor488 goat anti-mouse IgG (Invitrogen) counterstained with DAPI, and assessed using the Biorevo BZ-9000 (Keyence) or confocal microscopy (Olympus Japan, FV1000-D IX81, Tokyo, Japan).

Fluorescence *in-situ* hybridization (FISH)

The paraffin-embedded sections were deparaffinized and incubated in 2× SSC for 5 minutes at room temperature (RT), then heated in a microwave oven for 10 minutes and cooled to RT. The samples were subsequently incubated in 0.1% pepsin/0.1M HCl for 5 minutes at 37°C, washed with PBS, and dehydrated through a series of ethanol solutions. A human-specific genomic FISH probe labeled with Cy3 (Chromosome Science Labo, Sapporo, Japan) was then applied to the samples. The entire cover slide with the probe was denatured at 95°C for 10 minutes and then hybridized at 37°C overnight. The following day, the samples were washed with 50% formamide/2× SSC at 37°C for 20 minutes and then with 1×SSC at RT for 15 minutes. The

sections were double-stained with the other antibodies described above and counterstained with DAPI.

Real-time PCR

Total RNA was extracted from cardiac tissue and reverse transcribed using TaqMan reverse transcription reagents (Applied Biosystems, Stockholm, Sweden), and real-time polymerase chain reaction (RT-PCR) was performed with the ABI PRISM 7700 (Applied Biosystems)[7] system using pig-specific primers for vascular endothelial growth factor (VEGF) and basic fibroblast growth factor (bFGF). cDNA samples were prepared and assayed in triplicate. The average copy number of gene transcripts was normalized to that of glyceraldehyde-3-phosphate dehydrogenase (GAPDH) for each sample.

Statistical analysis

JMP software (JMP7.01, SAS institute Inc., Cary, NC) was used for all statistical analyses. Continuous values are expressed as the mean ± standard deviation. Within-group differences were compared with the Wilcoxon-Mann-Whitney U test and between-group differences with the Wilcoxon signed-rank test because the sample sizes are too small (just n=6 in each group and n=6 pairs) to allow checking of the assumptions of the unpaired and paired t-tests, respectively. A p-value < 0.05 was considered statistically significant.

Reference

1. Takahashi K, Tanabe K, Ohnuki M, Narita M, Ichisaka T, Tomoda K, Yamanaka S. Induction of pluripotent stem cells from adult human fibroblasts by defined factors. Cell. 2007; 131:861-872.

2. Jaroszeski MJ, Gilbert R, Heller R. Detection and quantitation of cell-cell electrofusion products by flow cytometry. Anal Biochem. 1994; 216:271-275.

3. Teramoto N, Koshino K, Yokoyama I, Miyagawa S, Zeniya T, Hirano Y, Fukuda H, Enmi J, Sawa Y, Knuuti J, Iida H. Experimental pig model of old myocardial infarction with long survival leading to chronic left ventricular dysfunction and remodeling as evaluated by PET. J Nucl Med. 2011; 52:761-768.

4. Teichholz LE, Kreulen T, Herman MV, Gorlin R. Problems in echocardiographic volume determinations: Echocardiographic-angiographic correlations in the presence or absence of asynergy. Am J Cardiol. 1976; 37:7–11.

5. Fukui S, Kitagawa-Sakakida S, Kawamata S, Matsumiya G, Kawaguchi N, Matsuura N, Sawa Y. Therapeutic effect of midkine on cardiac remodeling in infarcted rat hearts. Ann Thorac Surg. 2008; 85:562-570.

6. Zou Y, Liang Y, Gong H, Zhou N, Ma H, Guan A, Sun A, Wang P, Niu Y, Jiang H, Takano H, Toko H, Yao A, Takeshima H, Akazawa H, Shiojima I, Wang Y, Komuro I,

Ge J. Ryanodine receptor type 2 is required for the development of pressure overload-induced cardiac hypertrophy. Hypertension. 2011; 58:1099-1110.

7. Horiguchi K, Kitagawa-Sakakida S, Sawa Y, Li ZZ, Fukushima N, Shirakura R, Matsuda H. Selective chemokine and receptor gene expressions in allografts that develop transplant vasculopathy. J Heart Lung Transplant. 2002; 21:1090-1100.

Circulation
JOURNAL OF THE AMERICAN HEART ASSOCIATION

American Heart Association®

Mitral Valve Repair for Medically Refractory Functional Mitral Regurgitation in Patients With End-Stage Renal Disease and Advanced Heart Failure

Satoshi Kainuma, Kazuhiro Taniguchi, Takashi Daimon, Taichi Sakaguchi, Toshihiro Funatsu, Shigeru Miyagawa, Haruhiko Kondoh, Koji Takeda, Yasuhiro Shudo, Takafumi Masai, Mitsuru Ohishi and Yoshiki Sawa

Circulation. 2012;126:S205-S213
doi: 10.1161/CIRCULATIONAHA.111.077768
Circulation is published by the American Heart Association, 7272 Greenville Avenue, Dallas, TX 75231

Print ISSN: 0009-7322. Online ISSN: 1524-4539

Mitral Valve Repair for Medically Refractory Functional Mitral Regurgitation in Patients With End-Stage Renal Disease and Advanced Heart Failure

Satoshi Kainuma, MD; Kazuhiro Taniguchi, MD, PhD; Takashi Daimon, PhD; Taichi Sakaguchi, MD, PhD; Toshihiro Funatsu, MD, PhD; Shigeru Miyagawa, MD, PhD; Haruhiko Kondoh, MD, PhD; Koji Takeda, MD, PhD; Yasuhiro Shudo, MD; Takafumi Masai, MD, PhD; Mitsuru Ohishi, MD, PhD; Yoshiki Sawa, MD, PhD

Background—Information regarding patient selection for mitral valve repair for chronic kidney disease or end-stage renal disease (ESRD) with severe heart failure (HF) as well as outcome is limited.

Methods and Results—We classified 208 patients with advanced HF symptoms (Stage C/D) undergoing mitral valve repair for functional mitral regurgitation into 3 groups: estimated glomerular filtration rate ≥30 mL/min/1.73 m^2 (control group, n=144); estimated glomerular filtration rate <30 mL/min/1.73 m^2, not dependent on hemodialysis (late chronic kidney disease group, n=45), and ESRD on hemodialysis (ESRD group, n=19; preoperative hemodialysis duration 83±92 months). Follow-up was completed with a mean duration of 49±25 months. Postoperative (1-month) cardiac catheterization showed that left ventricular end-systolic volume index decreased from 109±38 to 79±41, 103±31 to 81±31, and 123±40 to 76±34 mL/m^2, in the control, late chronic kidney disease, and ESRD groups, respectively. Left ventricular end-diastolic pressure decreased, whereas cardiac index increased in all groups with no intergroup differences for those postoperative values. Freedom from mortality and HF readmission at 5 years was 18%±7% in late chronic kidney disease (P<0.0001 versus control, P=0.01 versus ESRD), and 64%±12% in ESRD (P=1 versus control) as compared with 52%±5% in the control group (median event-free survival, 26, 67, and 63 months, respectively).

Conclusions—Mitral valve repair for medically refractory functional mitral regurgitation in patients with advanced HF yielded improvements in left ventricular function and hemodynamics irrespective of preoperative renal function status. Patients with ESRD showed favorable late outcome in terms of freedom from mortality and readmission for HF as compared with those with late chronic kidney disease. Further studies are needed to assess the survival benefits of mitral valve repair in patients with ESRD and advanced HF. (***Circulation.*** **2012;126[suppl 1]:S205–S213.)**

Key Words: cardiomyopathy ■ chronic kidney disease ■ end-stage renal disease ■ functional mitral regurgitation ■ mitral valve repair

Heart failure and end-stage renal failure (ESRD) requiring dialysis are major health problems in Japan, as in the United States. Heart failure and chronic kidney disease (CKD) share a number of major risk factors, including hypertension and diabetes mellitus, and a substantial proportion of patients with advanced heart failure have impaired renal function.[1] Heart failure is the leading cause of mortality in patients with CKD or ESRD, whereas impaired renal function is strongly associated with poor outcomes in patients with chronic heart failure.[2] Moreover, kidney dysfunction per se is a risk factor for developing left ventricular (LV) remodeling and heart failure.[3,4]

Ischemic or nonischemic dilated cardiomyopathy is frequently complicated by functional mitral regurgitation (MR) as a consequence of LV remodeling progression. Medically refractory severe functional MR has a strong negative impact on survival of patients with CKD or ESRD and advanced heart failure. An increasing number of patients with ESRD has led to increased referrals of patients on dialysis for surgical repair of functional MR and other concomitant procedures.[5]

From the Department of Cardiovascular Surgery, Japan Labor Health and Welfare Organization Osaka Rosai Hospital, Sakai, Osaka, Japan (S.K., Ka.T., T.F., H.K.); the Departments of Cardiovascular Surgery (S.K., T.S., S.M., Ko.T., Ya.S., Yo.S.) and Geriatric Medicine and Nephrology (M.O.), Osaka University Graduate School of Medicine, Suita, Osaka, Japan; the Department of Biostatistics, Hyogo College of Medicine, Nishinomiya, Hyogo, Japan (T.D.); and Osaka Cardiovascular Surgery Research (OSCAR) group, Osaka, Japan (T.M.).

Presented at the 2011 American Heart Association meeting in Orlando, FL, November 13–17, 2011.

The online-only Data Supplement is available at http://circ.ahajournals.org/lookup/suppl/doi:10.1161/CIRCULATIONAHA.111.077768/-/DC1.

Correspondence to Yoshiki Sawa, MD, PhD, Department of Cardiovascular Surgery, Osaka University Graduate School of Medicine, 2-2-E1, Yamadaoka, Suita, Osaka 565-0871, Japan. E-mail Sawa@surg1.med.osaka-u.ac.jp

Circulation **is available at http://circ.ahajournals.org** **DOI: 10.1161/CIRCULATIONAHA.111.077768**

The EuroSCORE II calculator (www.euroscore.org/calc.html) shows that impaired renal function (ie, creatinine clearance <50 mL/min) off dialysis is a major risk factor for postoperative mortality in patients undergoing cardiovascular surgery, and patients with ESRD on dialysis are sometimes considered to be a relative contraindication to surgical intervention for medically refractory functional MR because other risk factors are commonly associated with this condition. Thus, surgical indication and patient selection for repair of functional MR in patients with CKD or ESRD are controversial, and risk stratification is not supported by the online STS Risk Calculator (http://209.220.160.181/STSWebRiskCalc261/de.aspx). Furthermore, long-term outcomes of patients with CKD or ESRD after surgery have not been sufficiently reported.[6]

We investigated the outcomes of patients with ESRD and advanced heart failure who underwent a restrictive mitral annuloplasty and other concomitant procedures for medically refractory severe functional MR.

Patients and Methods

Between August 1999 and July 2010, 226 consecutive patients with advanced cardiomyopathy were referred for surgical treatment of medically refractory severe or moderate-to-severe (regurgitant volume >30 mL/beat) functional MR and concomitant surgical procedures. Patients who underwent an emergency operation or with recent myocardial infarction (<3 months) were excluded; thus, 208 (166 men, 42 women; 65±10 years old) were analyzed in this retrospective study. Functional MR was caused by restrictive leaflet motion secondary to global severe LV dilatation (Type IIIb MR, Carpentier's classification) in all. Patients with organic MR, rheumatic mitral disease, or aortic valve disease were excluded. All had advanced (Stage C/D) heart failure symptoms and severe LV remodeling (ejection fraction [EF] <40%, end-systolic volume index >60 mL/m^2).

Our institutional ethical committees approved this study and written informed consent for the procedures was obtained from each patient before surgery.

Patient Stratification Based on Preoperative Renal Function

Estimated glomerular filtration rate was calculated by the Modification of Diet in Renal Disease equation.[7] Eight patients had an estimated glomerular filtration rate of >90 mL/min/1.73 m^2 (CKD Stage 1), 136 an estimated glomerular filtration rate of 60 to 89 or 30 to 59 mL/min/1.73 m^2 (CKD Stage 2 or 3), and 45 an estimated glomerular filtration rate of 15 to 29 or <15 mL/min/1.73 m^2 (CKD Stage 4 or 5: late CKD group). Nineteen patients had ESRD on hemodialysis (ESRD group), whereas 144 with CKD Stage 1 to 3 served as the control group.

Hemodialysis was introduced due to progression of diabetic nephropathy in 11, glomerular nephritis in 5, glomerular sclerosis in one, and unknown in 2 patients. Maintenance dialysis had been given for an average of 83±92 months (range, 3–300 months) before surgery. Patient characteristics for the 3 groups are presented in Table 1.

Echocardiography

Two-dimensional and Doppler transthoracic echocardiography examinations were performed before and 1 month after surgery, and annually thereafter. Measurements included LV end-diastolic dimension, LV end-systolic dimension, and LVEF. Systolic pulmonary artery pressure (PAP) was calculated by adding the value for right ventricular systolic pressure, derived from tricuspid regurgitation, to estimated right atrial pressure.[8,9] The inferior vena cava (IVC) dimension was measured through a subcostal approach. It was previously reported that IVC dimension is an accurate predictor of

Table 1. Patient Characteristics

Variables	Control (n=144)	Late CKD (n=45)	ESRD on HD (n=19)
Age, y*	64±10	68±9	64±6
Males	119 (83%)	33 (73%)	14 (74%)
Body surface area, m^2	1.65±0.18	1.62±0.17	1.57±0.16
NYHA class			
I	0 (0%)	0 (0%)	0 (0%)
II	13 (9%)	4 (9%)	1 (5%)
III	112 (78%)	32 (71%)	15 (79%)
IV	19 (13%)	9 (20%)	3 (16%)
Etiologies of cardiomyopathy*			
Ischemic cardiomyopathy	103 (72%)	34 (76%)	15 (79%)
Dilated cardiomyopathy	41 (28%)	11 (24%)	2 (11%)
Uremic cardiomyopathy	0 (0%)	0 (0%)	2 (11%)
Duration of preoperative HD			83±92
Comorbidity			
Hypertension	79 (55%)	28 (62%)	8 (42%)
Hyperlipidemia	58 (40%)	18 (40%)	4 (21%)
Diabetes	61 (42%)	24 (53%)	11 (58%)
Chronic obstructive lung disease	11 (8%)	3 (7%)	0 (0%)
Peripheral vascular disease	12 (8%)	5 (11%)	3 (16%)
Cerebral vascular accident	21 (15%)	8 (18%)	4 (21%)
Atrial fibrillation	45 (31%)	12 (27%)	6 (32%)
History of ventricular arrhythmia	26 (18%)	11 (24%)	3 (16%)
Previous cardiac surgery	13 (9%)	4 (9%)	1 (5%)
Previous CABG	9 (6%)	3 (7%)	0 (0%)
Previous PCI	61 (42%)	21 (47%)	4 (21%)
Laboratory examination			
Creatinine, mg/dL*	1.1±0.3	2.2±0.6	7.7±3.1
eGFR, mL/min/1.73 m^2*	57±19	23±5	7±3
Hemoglobin, g/dL*	13.1±2.1	11.3±2.2	10.4±1.4
Brain natriuretic peptide, pg/mL*	643±498	645±284	2335±1432
Medications			
Beta-blockers	96 (67%)	29 (64%)	10 (53%)
ACE inhibitors	46 (32%)	16 (36%)	3 (16%)
Angiotensin II receptor blockers	48 (33%)	13 (29%)	2 (11%)
Diuretics*	116 (81%)	34 (76%)	5 (26%)
Surgical data			
Mitral annuloplasty ring size			
24 mm	69 (48%)	27 (60%)	13 (68%)
26 mm	64 (44%)	17 (38%)	5 (26%)
28 mm	11 (8%)	1 (2%)	1 (6%)
Mitral annuloplasty alone	54 (38%)	21 (47%)	3 (16%)
Mitral annuloplasty+CABG	45 (31%)	12 (27%)	9 (47%)
Mitral annuloplasty+SVR	21 (15%)	6 (13%)	2 (11%)
Mitral annuloplasty+CABG+SVR	24 (17%)	6 (13%)	5 (26%)

Continuous variables are summarized as the mean±SD.

CKD indicates chronic kidney disease; ESRD, end-stage renal disease; HD, hemodialysis; NYHA, New York Heart Association; CABG, coronary artery bypass grafting; PCI, percutaneous coronary intervention; eGFR, estimated glomerular filtration rate; ACE, angiotensin-converting enzyme; SVR, surgical ventricular reconstruction.

*P<0.05 (one-way analysis of variance).